Polymer Brushes

Deutsche Ausgabe: DOI: 10.1002/ange.201607078
Internationale Ausgabe: DOI: 10.1002/anie.201607078

# Block Copolymer Brushes for Completely Decoupled Control of Determinants of Cell–Surface Interactions

*Inga Lilge and Holger Schönherr**

*Dedicated to Professor Curtis W. Frank on the occasion of his 70th birthday*

***Abstract:*** *The known determinants for cell–surface interactions, comprising biochemical cues, patterns, passivating functionality, and control of tether mechanical properties, are fully decoupled in tailored block copolymer brushes synthesized by surface-initiated atom transfer radical polymerization. Exploiting sequential polymerization of a passivating underlying polyacrylamide (PAAm) block with defined cross-linking followed by a second poly(acrylic acid) block, which can be conjugated with a selective adhesion peptide, hierarchically structured brushes that can be micro-patterned by soft lithography were obtained. The interaction of NIH 3T3 fibroblasts and PaTu 8988t pancreatic tumor cells with brushes that differed only in the stiffness of the hidden PAAm block or only in the peptide ligand, while keeping all other parameters constant, revealing profound differences in cell adhesion and morphology. In particular, cells could only attach well to stiff RGD presenting brushes.*

The interaction of cells with the extracellular matrix (ECM) as well as artificial microenvironments, such as designed biointerfaces and scaffolds in tissue engineering applications, is of paramount importance to understand and control cell behavior.[1] Cells sense and respond to a wide variety of external cues, including the nature, density, and spacing of adhesive ligands,[2] surface nano- and microtopography,[3] and the mechanical properties of the matrix.[4] In particular, matrix and substrate stiffness, or more precisely the mechanical properties of the molecular tethers of peptides affording focal adhesions[5] and the stress-stiffening in hydrogels,[6] constitute key parameters in regulating a range of cellular responses, including focal adhesion formation, changes in cell morphology, migration, proliferation, apoptosis, or differentiation, as evidenced by a variation in cell signaling and concomitantly gene expression.[7]

In the past, synthetic and natural materials, including PAAm and PEG gels, alginate, and agarose have been used to engineer substrates with defined mechanical properties that are functionalized with bioadhesive ligands to direct cell adhesion.[8] So far it remained a challenge to interrogate specifically the role of individual physical parameters on cell behavior, because of the concomitant change of other chemical and/ or physical parameters, when one parameter was changed.

Standard approaches vary the mechanical properties of bulk PAAm substrates that are coated with ECM components.[5,9] More recently, fibronectin patterns on PAAm hydrogels were used to analyze the influence of matrix rigidity on internal tension and its impact on remodeling the nucleus,[10] but also cardiac stem cell differentiation into different lineages.[1]

In the past decade, tailor-made polymer brushes have emerged as a promising alternative to the mentioned inert hydrogels.[11] Using controlled polymerization methods, defined substrate-independent architectures can be obtained that combine several functionalities.[12] Furthermore, the introduction of cross-linkers has been demonstrated to alter the mechanical properties in nanoscale thin coatings.[13] Despite the demonstrated applicability in cell studies and good control of brush composition and properties,[14] the decoupling of all known determinants for cell–surface interactions, comprising presented biochemical cues, patterns with a passivating functionality, and control of tether mechanical properties, has thus far been an unmet challenge.

Herein we show that carefully designed block copolymer brushes allow this challenge to be addressed successfully and that the tether mechanical properties are, at otherwise constant parameters, directly coupled to changes in adhesion and spreading area of NIH 3T3 fibroblasts and pancreatic tumor cells (PaTu 8988t). Similarly, the selectivity of the adhesion peptide RGD inducing integrin-mediated focal adhesions is shown.

The synthetic strategy of the cross-linked, biofunctionalized polymer brushes is shown in Scheme 1. Following the assembly of a monolayer of an initiator thiol for atom-transfer radical polymerization (ATRP) on a gold-coated substrate, surface-initiated ATRP of AAm in a monomer/water/methanol mixture containing CuBr and PMDETA was carried out.

The variation of mechanical properties of the initially polymerized PAAm block was realized by maintaining a constant concentration of AAm, while varying the concentration of the cross-linker bis-acrylamide (bisAAm) in the polymerization solution for each sample. Subsequently, the PAAm block was chain-extended by polymerizing a short PAA block, which in turn was functionalized by conjugation of a RGD peptide (GRGDS) via NHS/EDC chemistry (for detailed procedures, see the Supporting Information).

[*] I. Lilge, Prof. Dr. H. Schönherr
Physical Chemistry I and Research Center of Micro and Nanochemistry and Engineering (*Cμ*), University of Siegen
Adolf-Reichwein Strasse 2, 57076 Siegen (Germany)
E-mail: schoenherr@chemie.uni-siegen.de
Supporting information and the ORCID identification number(s) for the author(s) of this article can be found under: http://dx.doi.org/10.1002/anie.201607078.

  

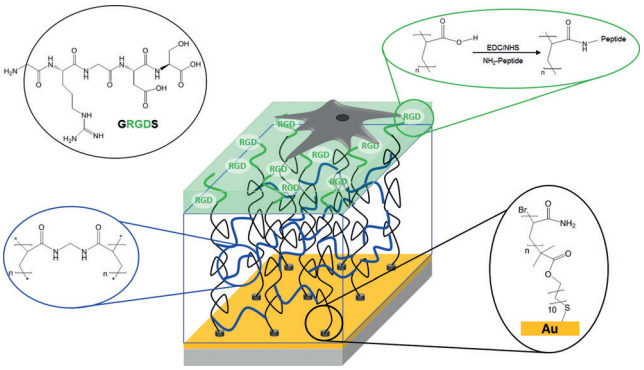


***Scheme 1.*** The biofunctional block-copolymer brush (PAAm/bisAAm-*b*-PAA) architecture. The crosslinking is implemented in the initially polymerized PAAm block, while the adhesion peptide RGD, conjugated to the subsequently polymerized PAA block, affords the signaling.

AFM imaging and ellipsometry measurements revealed that the initially synthesized cross-linked blocks were very uniform and could be adjusted to a dry film thickness (independent of the cross-link density) of $15.3 \pm 2.4$ nm. The mechanical properties were quantified in compression by AFM nanoindentation measurements with a colloidal force probe in water. The Young's modulus was determined according to the Hertz model from the slope of the force-indentation curve at low indentation depth ($< 15$ nm). A set of force curves is shown in Figure 1 A. The elastic moduli of polymer brushes varied from 3800 Pa for stiff substrates (prepared with 100 % bisAAm) and 600 Pa for soft substrates (0 % bisAAm; Figure 1 B). Concomitantly, the swelling ratios of the first block in aqueous environment were affected, which can be directly seen from the very different indentation depths under a constant load of for example, 10 nN in the force curves. The brushes with constant dry thickness of $15.3 \pm 2.4$ nm swelled in water up to 10-fold, which was observed for non-cross-linked brushes ($> 160$ nm). Similar results were obtained by Wu et al., who analyzed the dry and wet thickness of PAAm brushes grown on silicon wafers by ellipsometry.[15]

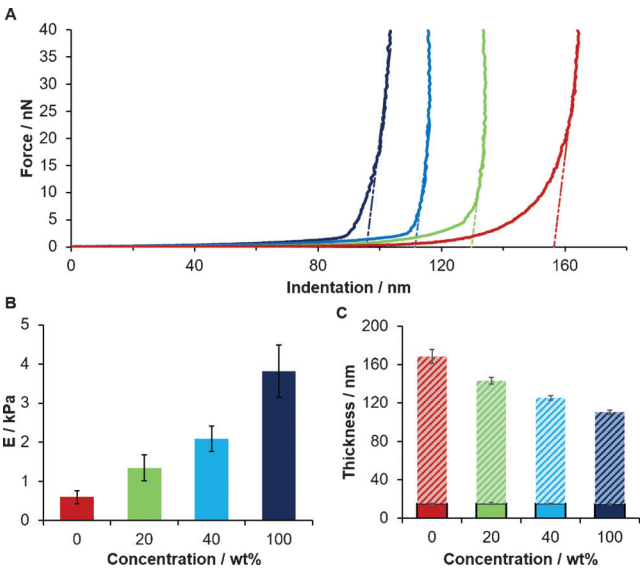


***Figure 1.*** AFM nanoindentation measurements measured with a glass bead on brushes in water at 25 °C (see the Supporting Information for details). A) Representative force curves as a function of the tip indentation. The color denotes the fraction of bisAAm in the feed: brown 0 %, green 20 %, light blue 40 %, dark blue 100 %). B) Elastic moduli of PAAm/bisAAm polymer with different cross-linking densities. C) Polymer brush thickness measured by ellipsometry in the dry state compared to the swollen thickness in water at 25 °C determined by the AFM nanoindentation measurements.

The initially synthesized block was then chain-extended with acrylic acid to obtain PAAm/bisAAm-*block*-PAA block copolymer brushes using a sequential polymerization strategy.[16] This second block was used to directly covalently conjugate a RGD peptide (GRGDS) or a RAD peptide (as negative control) via NHS/EDC chemistry.[14a]

The chain extension afforded a constant increase in dry film thickness of $5.5 \pm 1.4$ nm; hence under identical coupling conditions the subsequent conjugation is expected to result in virtually identical peptide concentrations. The successful functionalization of the block copolymer brushes obtained with RGD was confirmed by FTIR measurements of the as-prepared brushes as well as by XPS measurements of trifluoroacetic acid (TFAA)-labeled brushes (Supporting Information, Figures S1 and S2).[17] The TFAA labels the hydroxy group of the peptides; the corresponding XPS data confirmed to within the experimental error identical peptide coverage. The XPS spectra showed similar intensities of the F 1s signal at 689 eV for all films, despite different degrees of cross-linking in the underlying first block (Supporting Information, Table S1).

To evaluate the effects of the altered mechanical properties of the underlying PAAm block on cell adhesion, cells were seeded at a density of 12000 cells per $cm^2$ on the differently cross-linked block copolymer brushes. NIH 3T3 fibroblasts and pancreatic tumor cells (PaTu 8988t) were allowed to settle and adhere for 24 hours on brushes functionalized with RGD and RAD. The optical microscopy data revealed a decreasing cell density on the RGD-functionalized brushes with decreasing modulus for both cell lines. The images and the corresponding statistical analyses are shown in Figure 2.

There was no significant difference in cell adhesion on stiff substrates for both cell lines to that on tissue culture polystyrene (TCPS) surfaces. These results are fully consistent with the reported behavior of cells on hydrogels with varied mechanical properties by Pelham and Wang.[9] Control substrates that were conjugated with the nonadhesive peptide (RAD) instead of RGD exhibited minimal to no cell adhesion and spreading, which indicates the necessity of the RGD signal for integrin mediated focal adhesion formation.

Cells cultured on these substrates were stained for actin with phalloidin (red) and for the focal adhesions (paxillin, green) and analyzed by fluorescence microscopy, as shown in Figure 3. The projected cell area of both cell lines decreased with decreasing modulus. On the more rigid substrates (3800 Pa), cells were widely spread and appeared indistinguishable from those cultured on TCPS surfaces. In contrast, cells plated on soft substrates (600 Pa) poorly spread, lost

  

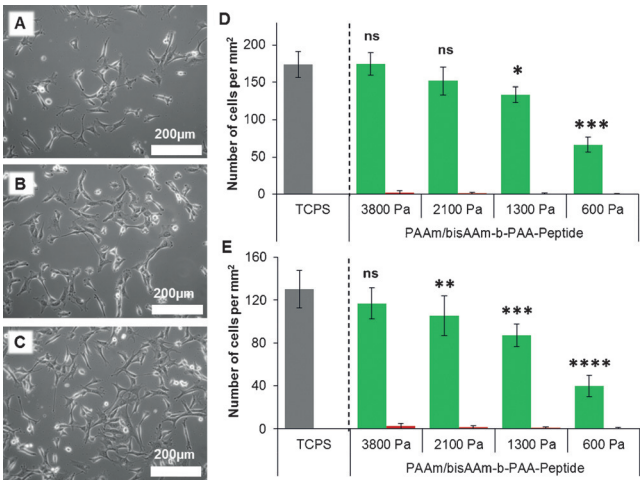


***Figure 2.*** A)–C) Optical microscopy images of NIH 3T3 cells on PAAm-*b*-PAA-RGD brushes with different moduli of the PAAm block (A: 600 Pa, B: 2100 Pa and C: 3800 Pa). D)–E) Number of cells per mm² (NIH 3T3 cells (D), PaTu 8988t cells (E)) on peptide-functionalized polymer brushes (green RGD, red RAD) compared to cells attached to a tissue culture poly styrene (TCPS) dish after 24 hours of culture. The measured cell number densities on softer PAAm-*b*-PAA-RGD brushes (1300 Pa and 600 Pa) were significantly lower than those observed on TCPS (*$p < 0.05$, **$p < 0.01$, ***$p < 0.001$, and ****$p < 0.0001$), but the number of cells on PAAm brushes (fraction of cross-linker during polymerization $> 0.2$) are not significant (ns).

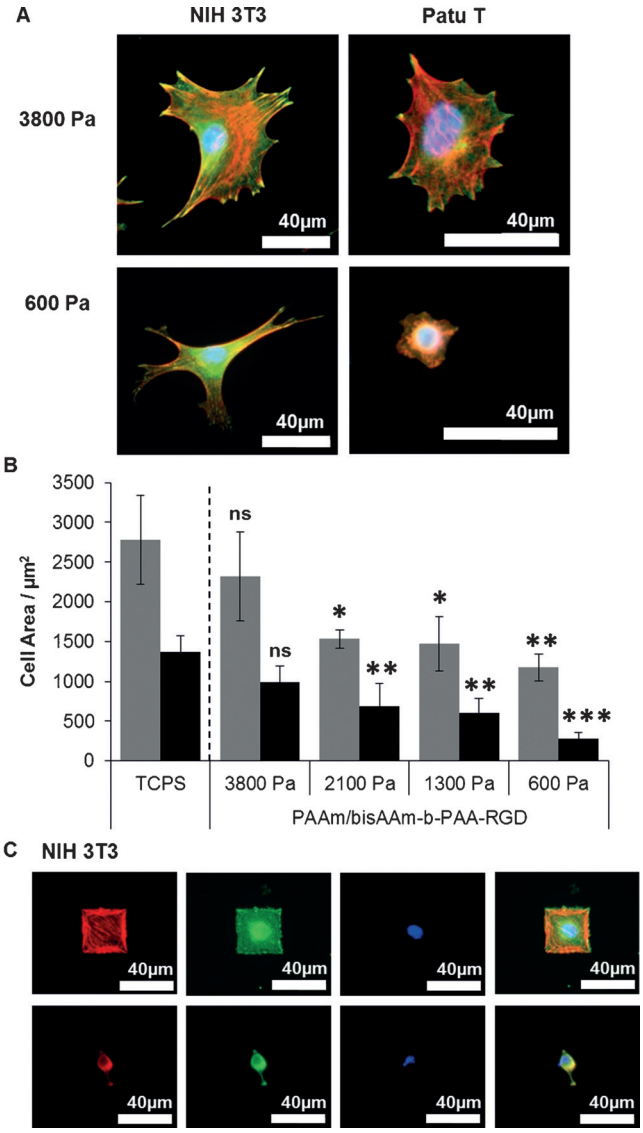


***Figure 3.*** A) Fluorescence microscopy images of NIH 3T3 and PaTu 8988t cells on PAAm-*b*-PAA-RGD brushes with different moduli of the PAAm block. The immunostaining method is included in the Supporting Information. B) The cell area of the cells on the polymer brushes compared to a tissue culture polystyrene (TCPS) dish after 24 h of culture (gray NIH3T3, black PaTu 8988t). For the fluorescence microscopy analysis, the cells were fixed, stained with Phalloidin-Rhodamine, Alexa 488, and DAPI for the cytoskeleton, paxillin, and nucleus, respectively. The measured cell areas on PAAm-*b*-PAA-RGD brushes with Young's moduli of 2100 Pa, 1300 Pa, and 600 Pa were significantly lower than those observed on TCPS (*$p < 0.05$, **$p < 0.01$, and ***$p < 0.0001$), except for the area of cells on 100% cross-linked PAAm brushes, which is not significant (ns). C) Representative fluorescence images of single NIH3T3 cells on square adhesive islands (area: 1600 μm²; top 3800 Pa, bottom 600 Pa) stained for actin (red), paxillin (green), and nuclei (blue) after culture for 6 h.

most of their well-organized stress fibers and became increasingly spindle-shaped. The actin cytoskeleton, which is not organized into stress fibers, shows instead a diffuse cortical actin organization that was relatively evenly distributed over the cell volume.

In cells on the rigid surfaces, stress fibers could be clearly observed as bundles stretching across the cells, which resembled the appearance of cells on the TCPS. The immunofluorescence staining of paxillin showed numerous large focal adhesions in clusters around the periphery of cells on stiff substrates and small dot-like focal adhesion clusters on soft substrates. These data show that the compliance of the substrate significantly affects the organization of the actin cytoskeleton, the formation of focal adhesions and results in a different morphology of the cells.

When cells are further confined by a 2D pattern, afforded by micro-contact printing of the initiator thiol (leaving a square area of 40 μm × 40 μm unfunctionalized), synthesis of a passivating PAAm brush ($d \approx 48$ nm), followed by backfilling of the initiator thiol to the previously unfunctionalized gold area and sequential synthesis of PAAm-*b*-PAA-RGD brushes with various cross-linking density, the differences in the formation of focal adhesions and morphology of the cells are enhanced. On the brush with a modulus of 3800 Pa, fibroblast cells spread and actin fibers aligned spanning the diagonal of the pattern (Figure 3 C). By contrast, on the brushes with identical structure and RGD adhesion peptide functionality, yet lower modulus of 600 Pa, hardly any cells can settle. The few remaining cells that could be imaged after fixation and staining were rounded and could not form focal adhesions. Unlike in previous reports,[18] we did not find evidence that these cells underwent apoptosis.

In conclusion, block copolymer brushes were shown to afford access to fully designed surfaces that enable independent and fully decoupled control of passivation, 2D micropatterning, peptide signaling, and mechanical properties to control cell adhesion. Both NIH 3T3 fibroblast and PaTu 8988t cells responded to differences in the tether mechanical

properties, which were hidden inside the brushes by altering their cytoskeleton organization and focal adhesion formation resulting in both altered cell densities and morphologies. Stiffer tethering facilitated more pronounced cell attachment compared to soft uncross-linked tethers. Cells failed to adhere and spread on non-functionalized PAAm brushes and block copolymer brushes functionalized with the non-adhesive RAD peptide, confirming the specificity of the interaction. The strategy shown herein may constitute the basis for further systematic investigations aiming at the decoupled investigation of the role of individual cues in integrin-mediated cell adhesion and beyond. Since polymer brushes can be employed as substrate-independent strategy for surface functionalization, the approaches reported above can be expanded to more relevant 3D structures, including 3D hydrogels and micro-compartmentalized matrices. Eventually this may lead to new insight and application for larger-scale cell culture and targeted cell therapy and tissue engineering.

## Acknowledgements

We thank Dr. Mareike Müller, Dr. Yvonne Voß, and Dipl.-Ing. Gregor Schulte for their constant support, stimulating discussions, and technical advice, as well as Dr. Jürgen Schnekenburger (Biomedical Technology Center of the Medical Faculty Münster, Germany), who kindly provided the cell lines. We also gratefully thank Dr. Daniel Wesner for the performance of the AFM measurements. The authors gratefully acknowledge financial support from the European Research Council (ERC project ASMIDIAS, Grant no. 279202) the Deutsche Forschungsgemeinschaft (DFG grant no. INST 221/87-1FUGG) and the University of Siegen.

**Keywords:** cell adhesion · micropatterning · nanomechanical properties · polymer brushes

**How to cite:** *Angew. Chem. Int. Ed.* **2016**, *55*, 13114–13117
*Angew. Chem.* **2016**, *128*, 13308–13311

[1] Y. Farouz, Y. Chen, A. Terzic, P. Menasché, *Stem Cells* **2015**, *33*, 1021–1035.

[2] a) A. S. Rowlands, P. A. George, J. J. Cooper-White, *Am. J. Physiol.-Cell Physiol.* **2008**, *295*, C1037–C1044; b) A. Chopra, V. Lin, A. McCollough, S. Atzet, G. D. Prestwich, A. S. Wechsler, M. E. Murray, S. A. Oake, J. Y. Kresh, P. A. Janmey, *J. Biomech.* **2012**, *45*, 824–831; c) E. A. Cavalcanti-Adam, A. Micoulet, J. Blümmel, J. Auernheimer, H. Kessler, J. P. Spatz, *Eur. J. Cell Biol.* **2006**, *85*, 219–224; d) S. P. Massia, J. A. Hubbell, *J. Cell Biol.* **1991**, *114*, 1089–1100.

[3] a) M. Arnold, E. A. Cavalcanti-Adam, R. Glass, J. Blümmel, W. Eck, M. Kantlehner, H. Kessler, J. P. Spatz, *ChemPhysChem* **2004**, *5*, 383–388; b) C. J. Bettinger, R. Langer, J. T. Borenstein, *Angew. Chem. Int. Ed.* **2009**, *48*, 5406–5415; *Angew. Chem.* **2009**, *121*, 5512–5522; c) K. Chung, J. A. Dequach, K. L. Christman, *Nano LIFE* **2010**, *1*, 63–77; d) D. Ning, B. Duong, G. Thomas, Y. Qiao, L. Ma, Q. Wen, M. Su, *Langmuir* **2016**, *32*, 2718–2723.

[4] a) D. E. Discher, P. A. Janmey, Y.-L. Wang, *Science* **2005**, *310*, 1139–1143; b) V. Vogel, M. P. Sheetz, *Nat. Rev. Mol. Cell Biol.* **2006**, *7*, 265–275; c) B. Geiger, J. P. Spatz, A. D. Bershadsky, *Nat. Rev. Mol. Cell Biol.* **2009**, *10*, 21–33; d) D. E. Ingber, *FASEB J.* **2006**, *20*, 811–827; e) S. Schmidt, M. Zeiser, T. Hellweg, C. Duschl, A. Fery, H. Möhwald, *Adv. Funct. Mater.* **2010**, *20*, 3235–3243.

[5] B. Trappmann, J. E. Gautrot, J. T. Connelly, D. G. T. Strange, Y. Li, M. L. Oyen, M. A. Cohen Stuart, H. Boehm, B. Li, V. Vogel et al., *Nat. Mater.* **2012**, *11*, 642–649.

[6] R. K. Das, V. Gocheva, R. Hammink, O. F. Zouani, A. E. Rowan, *Nat. Mater.* **2016**, *15*, 318–325.

[7] a) F. Guilak, D. M. Cohen, B. T. Estes, J. M. Gimble, W. Liedtke, C. S. Chen, *Cell Stem Cell* **2009**, *5*, 17–26; b) D. E. Discher, D. J. Mooney, P. W. Zandstra, *Science* **2009**, *324*, 1673–1677; c) P. A. Janmey, R. T. Miller, *J. Cell Sci.* **2011**, *124*, 9–18; d) J. Thiele, Y. Ma, S. M. C. Bruekers, S. Ma, W. T. S. Huck, *Adv. Mater.* **2014**, *26*, 125–147; e) A. K. Patel, M. W. Tibbitt, A. D. Celiz, M. C. Davies, R. Langer, C. Denning, M. R. Alexander, D. G. Anderson, *Curr. Opin. Solid State Mater.* **2016**, *20,* 202–211.

[8] a) D. Missirlis, J. P. Spatz, *Biomacromolecules* **2014**, *15*, 195–205; b) M. P. Lutolf, P. M. Gilbert, H. M. Blau, *Nature* **2009**, *462*, 433–441; c) E. Y. Tokuda, J. L. Leight, K. S. Anseth, *Biomaterials* **2014**, *35*, 4310–4318; d) A. J. Engler, S. Sen, H. L. Sweeney, D. E. Discher, *Cell* **2006**, *126*, 677–689; e) C. Cha, W. B. Liechty, A. Khademhosseini, N. A. Peppas, *ACS Nano* **2012**, *6*, 9353–9358; f) K. G. Robinson, T. Nie, A. D. Baldwin, E. C. Yang, K. L. Kiick, R. E. Akins, Jr., *J. Biomed. Mater. Res. Part A* **2012**, *100*, 1356–1367.

[9] R. J. Pelham, Y.-L. Wang, *Proc. Natl. Acad. Sci. USA* **1997**, *94*, 13661–13665.

[10] M. Versaevel, T. Grevesse, M. Riaz, J. Lantoine, S. Gabriele, *Methods Cell Biol.* **2014**, *121*, 33–48.

[11] a) N. Ayres, *Polym. Chem.* **2010**, *1*, 769–777; b) C. J. Fristrup, K. Jankova, S. Hvilsted, *Soft Matter* **2009**, *5*, 4623–4634; c) P. Akkahat, W. Mekboonsonglarp, S. Kiatkamjornwong, V. P. Hoven, *Langmuir* **2012**, *28*, 5302–5311; d) L. Li, J. Wu, C. Gao, *Colloids Surf. B* **2011**, *85*, 12–18; e) M. K. Gunnewiek, S. N. Ramakrishna, A. Di Luca, G. J. Vancso, L. Moroni, E. M. Benetti, *Adv. Mater. Interfaces* **2016**, *3*, 1500456.

[12] a) M. Navarro, E. M. Benetti, S. Zapotoczny, J. A. Planell, G. J. Vancso, *Langmuir* **2008**, *24*, 10996–11002; b) S. Tugulu, P. Silacci, N. Stergiopulos, H.-A. Klok, *Biomaterials* **2007**, *28*, 2536–2546.

[13] a) A. Li, E. M. Benetti, D. Tranchida, J. N. Clasohm, H. Schönherr, N. D. Spencer, *Macromolecules* **2011**, *44*, 5344–5351; b) I. Lilge, H. Schönherr, *Eur. Polym. J.* **2013**, *49*, 1943–1951.

[14] a) I. Lilge, H. Schönherr, *Polymer* **2016**, *98*, 409–420; b) I. Lilge, H. Schönherr, *Langmuir* **2016**, *32*, 838–847.

[15] T. Wu, K. Efimenko, P. Vlček, V. Šubr, J. Genzer, *Macromolecules* **2003**, *36*, 2448–2453.

[16] I. Lilge, M. Steuber, D. Tranchida, E. Sperotto, H. Schönherr, *Macromol. Symp.* **2013**, *328*, 64–72.

[17] A. Chilkoti, B. D. Ratner, D. Briggs, *Chem. Mater.* **1991**, *3*, 51–61.

[18] H. B. Wang, M. Dembo, Y. L. Wang, *Am. J. Physiol.-Cell Physiol.* **2000**, *279*, C1345–C1350.

Received: July 21, 2016
Revised: August 18, 2016
Published online: September 16, 2016

  